Visual Neuroscience (2018), **35**, e001, 12 pages.
Copyright © Cambridge University Press, 2018 0952-5238/18
doi:10.1017/S0952523817000360

RESEARCH ARTICLE

Differential epitope masking reveals synapse-specific complexes of TRPM1

MELINA A. AGOSTO, IVAN A. ANASTASSOV,[†] AND THEODORE G. WENSEL

Verna and Marrs McLean Department of Biochemistry and Molecular Biology, Baylor College of Medicine, Houston, Texas 77030

(RECEIVED July 8, 2017; ACCEPTED November 7, 2017)

Abstract

The transient receptor potential channel TRPM1 is required for synaptic transmission between photoreceptors and the ON subtype of bipolar cells (ON-BPC), mediating depolarization in response to light. TRPM1 is present in the somas and postsynaptic dendritic tips of ON-BPCs. Monoclonal antibodies generated against full-length TRPM1 were found to have differential labeling patterns when used to immunostain the mouse retina, with some yielding reduced labeling of dendritic tips relative to the labeling of cell bodies. Epitope mapping revealed that those antibodies that poorly label the dendritic tips share a binding site (N2d) in the N-terminal arm near the transmembrane domain. A major splice variant of TRPM1 lacking exon 19 does not contain the N2d binding site, but quantitative immunoblotting revealed no enrichment of this variant in synaptsomes. One explanation of the differential labeling is masking of the N2d epitope by formation of a synapse-specific multiprotein complex. Identifying the binding partners that are specific for the fraction of TRPM1 present at the synapses is an ongoing challenge for understanding TRPM1 function.

Keywords: TRPM1, ON bipolar cell, Epitope mapping, Epitope masking

Introduction

Rod and cone photoreceptor signaling to ON bipolar cells (ON-BPC) is mediated by a postsynaptic G protein-coupled transduction cascade. Following deactivation of the glutamate receptor mGluR6 in response to light (Nakajima et al., 1993; Masu et al., 1995; Dryja et al., 2005; Zeitz et al., 2005), the TRPM1 ion channel subunit is required for depolarization (Audo et al., 2009; Li et al., 2009; Morgans et al., 2009; Shen et al., 2009; van Genderen et al., 2009). In addition to mGluR6 and TRPM1, the leucine-rich repeat proteins nyctalopin (Bech-Hansen et al., 2000; Pusch et al., 2000; Gregg et al., 2003) and LRIT3 (Zeitz et al., 2013; Neuillé et al., 2014, 2015), the orphan GPCR GPR179 (Audo et al., 2012; Peachey et al., 2012; Ray et al., 2014), G proteins $G\alpha_o$ (Dhingra et al., 2000, 2002), $G\beta_3$ (Dhingra et al., 2012), and $G\beta_5$ (Chen et al., 2003; Rao et al., 2007), and GTPase accelerating protein RGS7 or RGS11 (Mojumder et al., 2009; Cao et al., 2012; Shim et al., 2012), are also required for normal ON-BPC function. The roles of some of these proteins, and the interactions among the cascade components, remain poorly understood.

TRPM1 has been reported to interact with nyctalopin (Cao et al., 2011; Pearring et al., 2011) and GPR179 (Orlandi et al., 2013; Ray et al., 2014), both of which also interact with mGluR6 (Cao et al., 2011; Orlandi et al., 2013), suggesting the formation of a large multiprotein signaling complex. However, unlike these other cascade components, which are localized specifically to the bipolar cell dendritic tips (Nomura et al., 1994; Masu et al., 1995; Morgans et al., 2006; Gregg et al., 2007; Peachey et al., 2012; Orlandi et al., 2013), TRPM1 is localized in bipolar cell bodies, dendrites, and axons (Morgans et al., 2009; Koike et al., 2010). This widespread distribution means that there is a large pool of TRPM1 that does not participate in the synaptic complex. In this study, we report TRPM1 monoclonal antibodies (mAbs) that preferentially detect the nonsynaptic pool of TRPM1 and identify the mAb epitope, which is likely masked by synapse-specific protein–protein interactions in the synaptic complex.

Materials and methods

Animals

WT C57BL/6 mice were purchased from the Baylor College of Medicine Center for Comparative Medicine. Trpm1 knock-out mice ($Trpm1^{tm1Lex}$; Lexicon Pharmaceuticals, The Woodlands, TX) were obtained from the European Mutant Mouse Archive and back-crossed to C57BL/6 for 15 generations before use (Agosto et al., 2014). Nob3 mice ($Grm6^{nob3}$) (Maddox et al., 2008) were obtained from The Jackson Laboratory. Absence of the $Pde6b^{rd1}$ allele was confirmed by genotyping as described (Gimenez & Montoliu, 2001), and absence of the $Crb1^{rd8}$ allele (Mattapallil et al., 2012) was confirmed by PCR amplifying and sequencing the surrounding region of genomic DNA.

Address correspondence to: Melina A. Agosto, Department of Biochemistry and Molecular Biology, BCM-125, Baylor College of Medicine, 1 Baylor Plaza, Houston, TX 77030. E-mail: agosto@bcm.edu

[†]Current address: Department of Ophthalmology, University of California, San Francisco, California 94143

https://doi.org/10.1017/S0952523817000360 Published online by Cambridge University Press

All procedures were approved by the Baylor College of Medicine Animal Care and Use Committee.

Cells

Spodoptera frugiperda clone 9 (Sf9) cells were maintained in InsectXpress medium (Lonza, Basel, Switzerland) supplemented with 10% heat-inactivated fetal bovine serum (FBS) (Sigma, St. Louis, MO) and 50 units/ml each of penicillin and streptomycin. Sf9 cells grown on coverslips in 24-well plates were infected with 50 μl passage 3 baculovirus. Human embryonic kidney 293 (HEK) cells (ATCC, Manassas, VA) were maintained in Dulbecco's modified Eagle medium (Corning, Corning, NY) supplemented with 10% FBS (Hyclone, Logan, UT or Sigma, St. Louis, MO). HEK cells in 6-well plates were transfected with 1–3 μg plasmid DNA using Lipofectamine 2000 (ThermoFisher, Waltham, MA) according to the manufacturer's instructions.

Primary antibodies

TRPM1: Purification of full-length TRPM1, generation of mAbs at the Baylor College of Medicine Monoclonal Antibody/Recombinant Protein Expression Core, and protein G purification of mAbs from hybridoma cultures, were previously described (Agosto et al., 2014). Isotyping was performed by ELISA at the core facility. Purified 545H5 and 274G7 were diluted to 1 μg/ml for western blotting and 5 μg/ml for immunofluorescence (IF); purified 1109F9, 717G8, and 803G4 were used at 1 μg/ml for westerns with recombinant TRPM1, 5 μg/ml for westerns with retina tissue, and 5 or 20 μg/ml for IF. For some epitope mapping experiments, TC supernatants were used, diluted to 15–35%. *mGluR6*: Full-length mouse mGluR6 was purified and complexed with amphipol as described for TRPM1 (Agosto et al., 2014), except protein and amphipol were mixed in a 1:3 (w/w) ratio. Mice were immunized with protein/amphipol complexes at the Baylor College of Medicine Monoclonal Antibody/Recombinant Protein Expression Core facility. Resulting mAbs were purified as described for TRPM1 antibodies, and clone 312 was used in westerns at 1–2 μg/ml. In some experiments, the intermediate polyclonal mouse serum was used for westerns, diluted 1:1000. Validation of the specificity of the mGluR6 band obtained with this antibody, using retina lysates from WT and nob3 mice, which do not express mGluR6 (Maddox et al., 2008), is shown in Fig. 7Bii. *Myc tag*: c-Myc clone 9E10 hybridomas were obtained from the Developmental Studies Hybridoma Bank (The University of Iowa), and the antibody was purified as described for TRPM1 antibodies and diluted to 1 μg/ml for westerns. The following antibodies were additionally used for westerns: *actin*, Santa Cruz mouse monoclonal (#sc-58673), 0.5–1 μg/ml, or Cell Signaling mouse monoclonal 8H10D10 (#3700), 1:500–1:4000; *PSD-95*, UC Davis/NIH NeuroMab Facility mouse monoclonal K28/43 (#75-028), 0.5–1 μg/ml; *ribeye/CtBP2*, BD Transduction mouse monoclonal (#612044), 0.13 μg/ml; *PDI*, Cell Signaling rabbit monoclonal C81H6 (#3501), 1:1000; *GST*, Thermo Fisher mouse monoclonal 8-326 (#MA4-004), 0.3 μg/ml; and for IF: *ribeye*, Synaptic Systems rabbit polyclonal anti-ribeye A-domain (#192-103), 4–5 μg/ml.

Confocal immunofluorescence microscopy and image processing

Mice were euthanized and whole eyes were fixed in 4% PFA in PBS for ~45–60 min, washed extensively in PBS, then cryoprotected in 30% sucrose in PBS overnight at 4°C. After removing the cornea and the lens, eyecups were embedded in OCT. For some experiments, eyecups were dissected in a fixing solution, prior to cryoprotection. Blocks were sectioned at 8–18 μm thickness and adhered either to Superfrost Plus slides (VWR, Radnor, PA or Fisher, Waltham, MA) or coverslips coated with 100 μg/ml poly-D-lysine. Sections were stored at –20°C.

Sections were optionally postfixed in 4% PFA for 10 min, washed three times in PBS, and blocked for 1–2 h at room temperature (RT) in PBS with 10% donkey serum, 5% BSA, and 0.2% Triton X-100. For some experiments, the blocking buffer consisted of PBS with 2% goat serum, 2% fish skin gelatin, 2% BSA, and 0.5% Triton X-100. Samples were incubated overnight at 4°C with primary antibodies diluted in the blocking buffer, then washed in PBS at RT. Samples were incubated at RT for 2 h with secondary antibodies [donkey anti-mouse-Alexa488, goat anti-mouse-Alexa555 and donkey anti-rabbit-Alexa488, or goat anti-mouse-IgG2B-Alexa555 and goat anti-mouse-IgG1-Alexa488 (Invitrogen/Thermo Fisher, Waltham, MA)] diluted to 8–10 μg/ml in the blocking buffer, then were washed in PBS and mounted with Prolong Gold (Molecular Probes/Thermo Fisher, Waltham, MA).

Sf9 cells on coverslips were fixed and labeled at ~45 h post-infection as described previously (Agosto et al., 2014), with 5 μg/ml each of 545H5 and 1109F9, followed by 2 μg/ml goat anti-mouse-IgG2B-Alexa555 and goat anti-mouse-IgG1-Alexa488 (Invitrogen/Thermo Fisher).

Images were acquired with a TCS-SP5 laser scanning confocal microscope (Leica) using a 63× oil immersion objective (Leica, HC PL APO CS2 63.0×, numerical aperture 1.40). Images are single optical sections. Alexa 555, Alexa 488, and DAPI were detected in a sequential mode with a 543 nm HeNe laser, 488 nm argon laser, and 405 nm diode laser, respectively, with imaging parameters set to avoid crosstalk between the channels. Images were acquired with few or no saturated pixels. For qualitative figures, images were processed in ImageJ (NIH) and/or Photoshop (Adobe) to adjust the minimum and maximum input levels, maintaining a linear slope. For quantification of relative outer plexiform layer (OPL) labeling, the intensities of regions of interest (ROIs) in raw images (240.5 nm/pixel resolution) were measured in ImageJ. ROIs were drawn such as to encompass the cell bodies or the OPL/dendrites, while avoiding blood vessels. Two background boxes were drawn, one in the outer nuclear layer and one in the inner nuclear layer (INL) or inner plexiform layer below the bipolar cell body staining; each ROI-integrated intensity was background corrected by subtracting the mean intensity/pixel of the two background boxes multiplied by the ROI area. The percentage signal in the dendritic tips was then calculated as 100 × OPL/(OPL + cell bodies).

For the quantification of individual dendritic tip puncta, cell bodies in raw images (40.1 or 48.1 nm/pixel resolution) were masked out with a line drawn between the OPL and INL. Image thresholding was used to detect the puncta, and ROIs were defined with "Analyze Particles" in ImageJ, using the same parameters for all images. Particles with less than 20 pixels were ignored, and some particles which were obviously not dendritic tip puncta were manually removed. ROIs were then applied to raw images to measure the area and mean intensity. The mean intensity of the image in the INL/cell body region was determined using the inverse of the mask used for the puncta, with blood vessels manually excluded. Both the puncta and INL mean values were corrected by subtracting the mean background value determined as above, and the puncta were normalized by dividing by the mean INL intensity. Mean values were used, rather than integrated density, because the thresholding procedure resulted in smaller ROIs for dimmer puncta, likely underestimating their area. Puncta from 11–12 images were combined for each mAb, and very large spots with area >1.5 × interquartile range were discarded.

https://doi.org/10.1017/S0952523817000360 Published online by Cambridge University Press

Ratio images were computed in Mathematica (Wolfram, Champaign, IL) by first scaling raw images for the red and green channels to intensity values between 0 and 1 using the *ImageAdjust* function and then calculating for each pixel the ratio red/(red + green) or green/(red + green), with divisions 0/0 replaced with 0. Pseudocoloring was applied in ImageJ using the "ICA" color scheme.

Western blotting

Proteins were separated by SDS-PAGE (Laemmli, 1970). For the detection of membrane proteins including TRPM1, samples were mixed with reducing the SDS loading buffer and loaded without heating. Proteins were electrophoretically transferred to nitrocellulose membrane in 25 mM Tris, 192 mM glycine, blocked in 5% milk in TBST (50 mM Tris, 150 mM NaCl, 2% Tween-20, pH ~ 8.4), and blotted with primary antibodies diluted in the blocking solution. The blots were then either incubated with donkey anti-mouse-IRdye800CW (LI-COR, Lincoln, NE) diluted to 0.1 μg/ml for typical westerns or 0.05 μg/ml for quantitative westerns and scanned using an Odyssey infrared scanner (LI-COR) or incubated with horseradish-peroxidase conjugated anti-mouse, anti-mouse-light-chain, or anti-rabbit (Jackson ImmunoResearch, West Grove, PA) 0.16 μg/ml followed by HyGLO (Denville Scientific, Holliston, MA) or SuperSignal West Pico (Thermo, Waltham, MA) chemiluminescent substrate, and exposed to film.

Bands on infrared fluorescence scans of quantitative westerns were analyzed in ImageQuant (GE) by measuring the integrated intensity of a box around the band, subtracted by an adjacent background box of equal size.

Epitope mapping

TRPM1 fragments (large fragments 1–502, 482–875, 810–1150, and 1126–1622, and smaller fragments as indicated in the figure legends) were cloned into a modified pGEX-2TK vector (Harper et al., 1993) to produce an in-frame fusion to the C-terminus of GST following the thrombin and kinase sites. GST fusion proteins were expressed in BL21(DE3)pLysS *E. coli* (EMD Millipore Novagen, Burlington, MA) in terrific broth. Cultures were grown to OD_{600} 0.2–0.6, induced with 100 or 190 μM isopropyl β-D-1-thiogalactopyranoside (IPTG), and grown for 4–5 h at 25–27°C. The OD was measured again, and equal numbers of cells were pelleted and resuspended in 25 mM Tris, 200 mM NaCl, 15 mM EDTA, pH 8.1, with Complete protease inhibitors (Roche, Basel, Switzerland), and boiled in reducing SDS sample buffer. Material equivalent to 200 μl at OD_{600} = 0.7 were loaded in each lane for SDS-PAGE.

TRPM1 splice variant cloning and constructs

TRPM1 was amplified from 15 ng mouse retina cDNA (Gilliam & Wensel, 2011) using KOD hot-start DNA polymerase (EMD Millipore Novagen) and primers 1R (5′-ATGGTCTGGCTGTTGAGTGC TTG-3′) and either 1F (5′-ACTCTCTTACCTCAGCTGACCAG-3′) or 2F (5′-TGTCAGCAAACACACCCAGAGCTAC-3′). PCR products were gel purified, A-tails were added by incubating with Taq polymerase and 2 mM dATP for 30 min at 70°C, and tailed products were cloned into the pCR2.1-TOPO-TA vector (Invitrogen/ThermoFisher) following the manufacturer's instructions. Clones were screened with BfaI, XhoI, and EcoRI (EcoRI and XhoI cut inside exon 19, and EcoRI and BfaI cut inside the 18 nt extension of exon 22L). For expression in insect cells, TRPM1 open reading frames were cloned into pFb1 (Invitrogen/ThermoFisher) SpeI/KpnI sites with C-terminal 1D4 tags (Mackenzie et al., 1984) and baculovirus made as previously described (Agosto et al., 2014). For expression in HEK cells, the mouse TRPM1 variant C with an N-terminal Myc tag and a C-terminal 1D4 tag was cloned into pCDNA3.1 (Invitrogen/ThermoFisher) KpnI/NotI. Human TRPM1 (kindly provided by Craig Montell, University of California, Santa Barbara) (Xu et al., 2001) with an N-terminal Myc tag was cloned into pCDNA3.1 KpnI/XhoI; the human TRPM1 variant used is homologous to the mouse isoform C, except it begins in exon 4 at the methionine corresponding to a.a. 117 in the mouse protein. This is likely not a full-length human protein, as upstream coding exons were subsequently identified (Oancea et al., 2009), yielding a variant with the N-terminus similar to that of mouse TRPM1; however, it covers 93% of the full-length protein including both antibody epitopes.

Retina fractionation

The fractionation protocol was developed based on previously published protocols for isolation of synaptosomes from rat retina (VanGuilder et al., 2008), bovine retina (Dhingra et al., 2004), and rat brain (Scott et al., 2003). 18–20 WT C57BL/6 mice were used for each experiment. Retinas were collected into cold PBS and washed by cycles of low-speed centrifugation and resuspension three times in the PBS. Retinas were then washed three times in cracking buffer [CB; 25 mM Tris, 300 mM sucrose, 15 mM EDTA, 2 mM $MgCl_2$, pH 8.1, 1× Complete protease inhibitor (Roche)], vortexing gently each time for ~30 s to shear off outer segments. Retinas were homogenized by pipetting up and down in 20 μl/retina CB, followed by 100 passes through a 23 G needle and 40 passes through a 26 G needle. The lysate was centrifuged at 800 × *g* for 12 min, yielding the nuclear pellet, which was resuspended in 20 μl/retina CB. The supernatant was centrifuged again at 800 × *g* for 6 min to remove any traces of the pellet, yielding the postnuclear supernatant (PNS). The PNS was centrifuged at 17,000 × *g* for 15 min and the pellet was washed in 20 μl/retina CB and centrifuged again to remove the residual supernatant, then resuspended in 5 μl/retina CB, yielding the synaptosome fraction. Meanwhile, the 17,000 × *g* supernatant was centrifuged at 100,000 × *g* for 2 h, yielding the soluble fraction (supernatant), and the microsome pellet, which was homogenized with a 23 G needle in 5 μl/retina CB. Fractions were quantified using the BCA protein assay (Pierce/ThermoFisher, Waltham, MA).

RNA-seq data analysis

Data from (Farkas et al., 2013) was obtained using the UCSC Genome Browser (https://oculargenomics.meei.harvard.edu/retinal-transcriptome). For other data sets, NCBI GEO sequence read archives were queried using the NCBI Sequence Read Archive Nucleotide BLAST. Queries consisted of 48-nt sequences (24 nt on each side of the splice junction), and hits with at least 28 consecutive matches were counted. The following data sets were used: human retina (combined three peripheral retina samples and three macular retina samples from accession number GSE94437, Dwight Stambolian, University of Pennsylvania), and WT C57BL/6 mouse retina (combined WT retina samples from GSE84927 (Mustafi et al., 2016), three biological replicates; and GSE29752 (Mustafi et al., 2011), one sample).

https://doi.org/10.1017/S0952523817000360 Published online by Cambridge University Press

Sequence analysis

Multisequence alignments were performed using ClustalX (Larkin et al., 2007) or Clustal Omega (Sievers et al., 2011).

Statistical analysis

Data sets were subjected to statistical tests as described in the figure legends, using Prism (GraphPad, La Jolla, CA).

Results

Specificity of TRPM1 mAbs

To study native TRPM1 in the retina, we generated mAbs using full-length purified TRPM1, and we previously reported validation of clones 274G7 and 545H5 in western blots of retinas from Wild-type (WT) and Trpm1 knockout mice (Agosto et al., 2014). Here, we further show the specificity of these and additional clones, in both immunofluorescence (IF) microscopy and western blots of mouse retina tissue (Fig. 1). All clones were isotyped, revealing both IgG1 and IgG2b clones (see below).

Differential labeling of bipolar cell dendritic tips with TRPM1 mAbs

In IF microscopy experiments, some mAbs labeled both the dendritic tip puncta and cell bodies, as expected from results with polyclonal antibodies (Morgans et al., 2009; Koike et al., 2010), while others labeled primarily cell bodies, with reduced signal in the dendritic tips (Fig. 2A). To quantitate this phenomenon, the relative intensity of outer plexiform layer (OPL) and cell body labeling in confocal images was measured for four clones (Fig. 2B). Clones 545H5 and 274G7 were similar, with ~30% of the total signal originating from the OPL. Clones 1109F9 and 717G8 both had significantly less relative labeling of the dendritic tips, with ~15–20% of the signal in the OPL. As a complimentary approach, we also

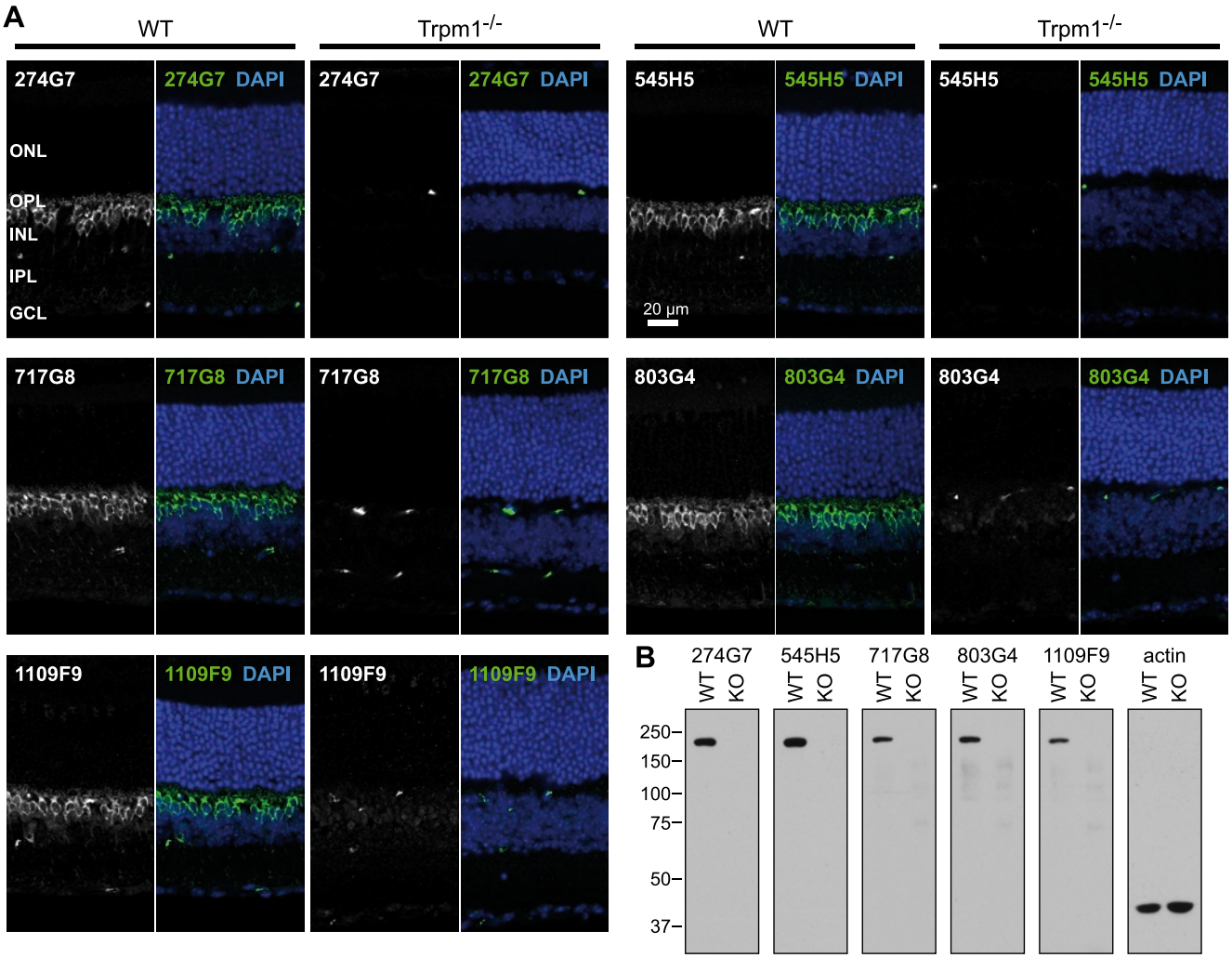


Fig. 1. Specificity of antibody clones. (**A**) Retina sections from WT and Trpm1 KO mice were labeled with TRPM1 mAbs, followed by anti-mouse-Alexa488. TRPM1 labeling in bipolar cells is observed specifically in the WT mice. Blood vessels, which are labeled by the anti-mouse secondary antibody, are detected in both WT and KO samples. ONL, outer nuclear layer; OPL, outer plexiform layer; INL, inner nuclear layer; IPL, inner plexiform layer; GCL, ganglion cell layer. (**B**) Retina postnuclear supernatants prepared from WT and KO mice were blotted with TRPM1 or actin antibodies, followed by horseradish-peroxidase-conjugated light-chain-specific antimouse. Approximately 60 μg/lane were loaded for TRPM1 blots and 40 μg/lane for actin.

https://doi.org/10.1017/S0952523817000360 Published online by Cambridge University Press

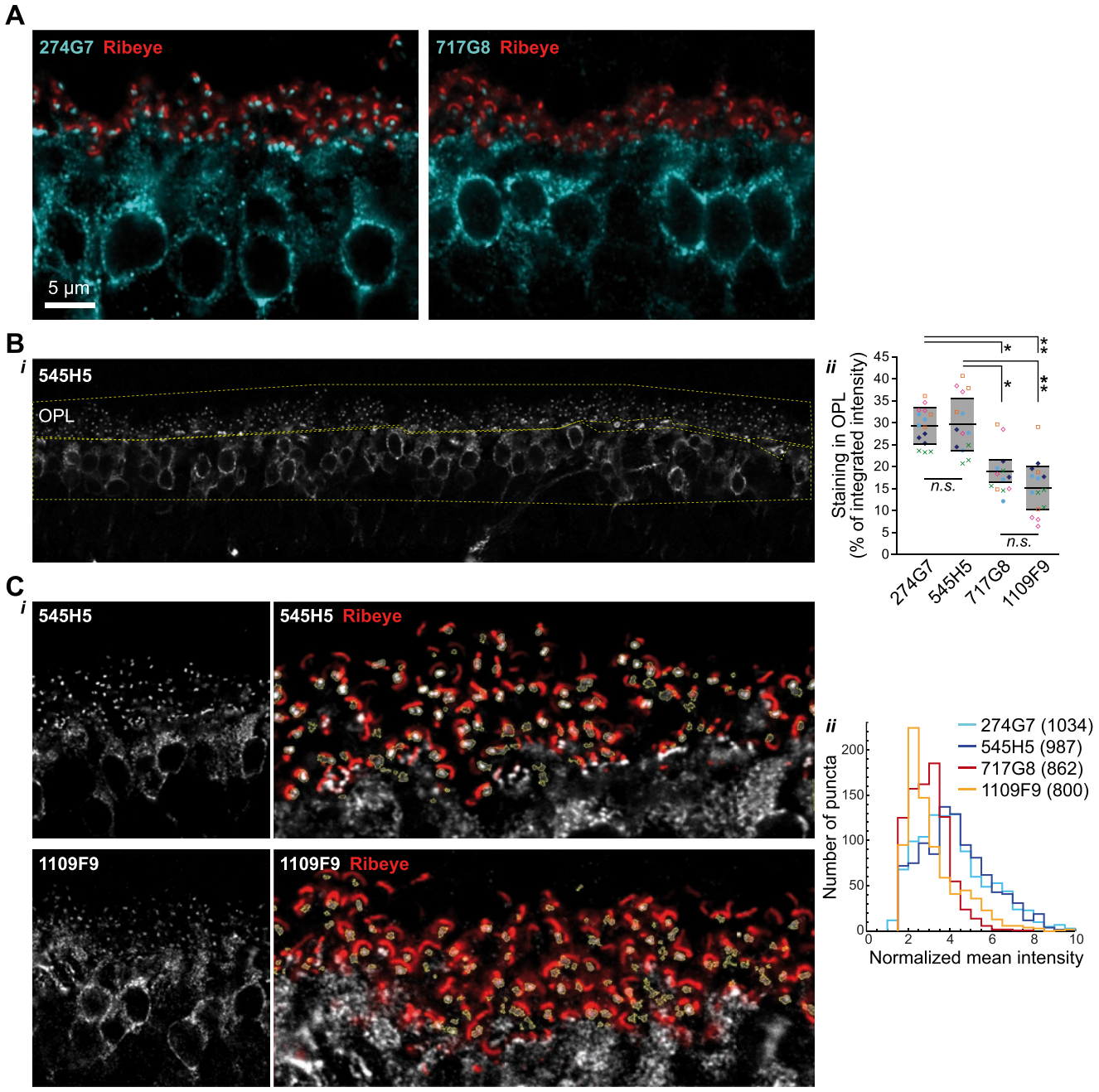


Fig. 2. Differential labeling of TRPM1 with different mAbs. (**A**) 274G7 (left) labels bipolar cell bodies and dendritic tip puncta, as expected for TRPM1, while labeling of dendritic tips with 717G8 (right) appears to be reduced. Samples were co-stained with ribeye antibody (red) to show the presence of similar numbers of synapses in both images. (**B**) Quantification of relative labeling in cell bodies and dendritic tips. ROIs encompassing the cell bodies and dendritic tips were drawn as shown in the example image (i, yellow lines). (ii) In samples labeled with 1109F9 and 717G8, significantly less of the total TRPM1 intensity was present in the dendritic tips. For each clone, 2–3 images were acquired from each of five eyes, from five different animals. Points show technical replicates, with biological replicates represented by different symbols. Horizontal lines and shaded areas indicate means ±S.D. of the means from each eye only, not including technical replicates. One-way ANOVA with Tukey's Multiple Comparison Test was applied to the means from each eye only: $*P < 0.05$; $**P < 0.001$; n.s., not significant, $n = 5$. (**C**) Quantification of individual dendritic tip puncta. (i) Example images used for quantification, with ROIs (yellow lines) and ribeye counterlabel (red), shown on the right in magnified views of the OPL region. (ii) Distributions of mean puncta intensities normalized by cell body labeling. The number of puncta included in each distribution is shown in the legend. 11–12 images from four animals were analyzed for each clone.

quantified the intensities of individual dendritic tip puncta in higher-magnification images (Fig. 2C), normalized by the signal in the inner nuclear layer (INL) region of the image. This procedure likely undercounts poorly labeled puncta, as dim puncta were sometimes missed by the detection procedure (see Materials and methods). Nevertheless, the distribution of puncta intensities for 1109F9 and 717G8 was similar and shifted toward lower values, compared to 545H5 and 274G7, consistent with the results from quantification of the whole OPL.

https://doi.org/10.1017/S0952523817000360 Published online by Cambridge University Press

Because the appearance of labeling in the dendritic tips can be affected by the orientation of the tissue during sectioning and confocal imaging, we also performed double labeling experiments, taking advantage of the fact that some of the clones are of different isotypes (see Fig. 4C). In sections co-labeled with 545H5 (IgG2B) and 1109F9 (IgG1), the dendritic tips of both the rod and cone ON bipolar cells are labeled more efficiently with 545H5 (Fig. 3A). Images constructed from the ratio of the 545H5 signal to the total signal for each pixel show that even in images where the cell bodies have more signal in the 1109F9 channel, the majority of the signal at the dendritic tips is in the 545H5 channel. Similarly, in sections co-labeled with 274G7 (IgG1) and 803G4 (IgG2B), the dendritic tips are labeled more efficiently with 274G7 (Fig. 3B). To confirm that the observed staining patterns were not due to different accessibilities of IgG2b and IgG1 isotypes, we also co-labeled sections with 545H5 and 274G7, which both efficiently label the dendritic tips (Fig. 3C); in these samples, the relative intensity of the signal in the 545H5 and 274G7 channels were similar in the cell bodies and dendritic tips. These results indicate that some mAbs preferentially detect different pools of TRPM1 molecules.

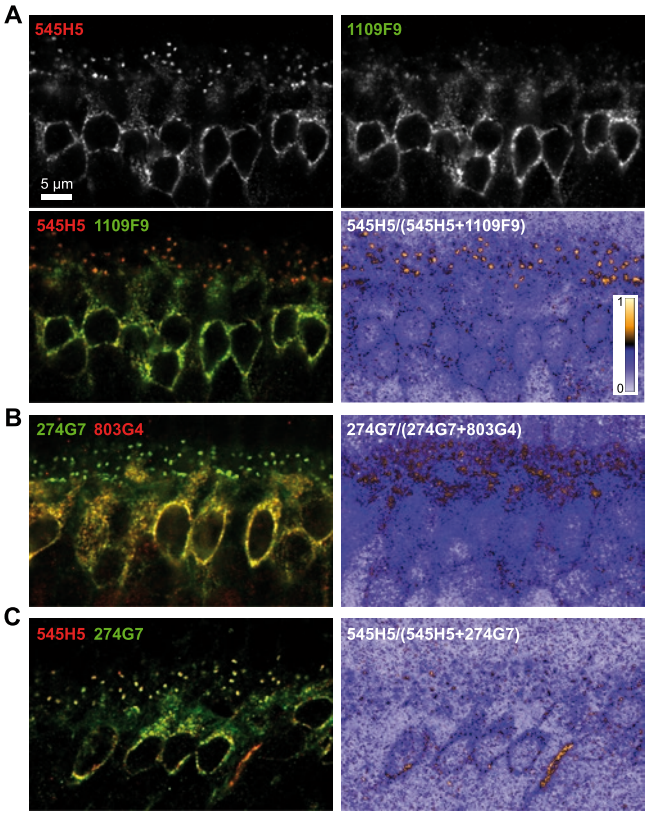
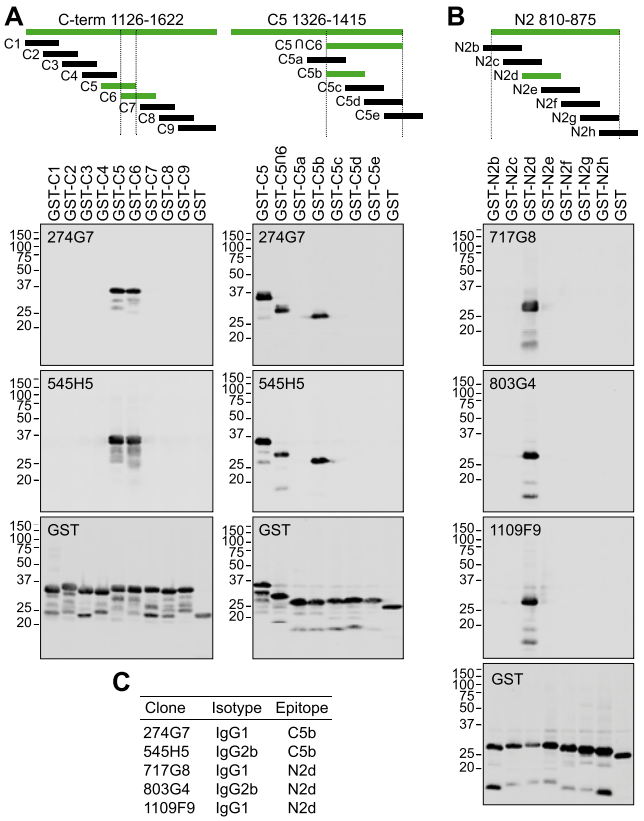


Fig. 3. (**A**) Retina sections were double-labeled with 545H5 (IgG2b, red) and 1109F9 (IgG1, green), followed by isotype specific secondary antibodies. The relatively poor labeling of the dendritic tips by 1109F9 is highlighted in an image computed from the ratio of the 545H5 signal to the total signal for each pixel. (**B**) Retina sections were double-labeled with 274G7 (IgG1, green) and 803G4 (IgG2b, red). The relatively poor labeling of the dendritic tips by 803G4 is shown in an image computed from the ratio of the 274G7 signal to the total signal for each pixel. (**C**) As a control, retina sections were double-labeled with 545H5 (IgG2b, red) and 274G7 (IgG1, green). The dendritic tips are similarly labeled in both channels.

MAb epitope mapping

To begin to decipher the differences between the mAbs, we performed epitope mapping experiments. Fragments of TRPM1 were expressed as GST fusions in *E. coli*, and cell lysates were subject to western blotting with GST and TRPM1 mAbs. Following preliminary experiments with large fragments, which indicated the general region of binding (not shown), the epitopes were further narrowed down using small overlapping fragments (Fig. 4A and 4B). All five of the tested clones bind within one of two 20-aa regions: an epitope in the C-terminal arm (C5b, ATPGRSRLALEGPLSTELRP), and an epitope in the N-terminal arm near the transmembrane domain (N2d, EDGKEKEEENVDANADAGSR) (see diagram, Fig. 5B). Isotyping revealed IgG1 and IgG2b clones for both epitopes



Clone	Isotype	Epitope
274G7	IgG1	C5b
545H5	IgG2b	C5b
717G8	IgG1	N2d
803G4	IgG2b	N2d
1109F9	IgG1	N2d

Fig. 4. Epitope mapping. TRPM1 fragments fused to the C-terminus of GST were expressed in *E. coli* and subjected to western blotting with TRPM1 mAbs. (**A**) The epitope of mAbs which were initially found to bind in a large fragment consisting of the entire C-terminal arm (a.a. 1126–1622) (not shown) was narrowed down by expressing overlapping 90-a.a. fragments. 274G7 and 545H5 detected both C5 and C6 (Left), indicating a probable epitope in the region of overlap between these two fragments (C5∩C6). The epitope was further narrowed down to the 20-a.a. C5b fragment (a.a. 1376–1395) by expressing overlapping fragments covering C5∩C6 (Right). (**B**) After initial experiments indicated binding of some mAbs to two large fragments—one containing approximately the second half of the N-terminal arm (a.a. 482–875) and one containing the transmembrane domain (a.a. 810–1150)—and therefore a probable epitope in the region of overlap (not shown), the epitope was narrowed down to the 20-a.a. N2d fragment (a.a. 826–845) by expressing overlapping fragments covering a.a. 810–875. All amino acid numbers refer to the position in NP_001034193.2 (isoform C). Fragments detected by TRPM1 mAbs are shown in green. Expression of all constructs used for epitope mapping was confirmed with an antibody against the GST tag [bottom panels in (**A**) and (**B**)]. (**C**) Summary of mAb clone isotypes and epitopes.

https://doi.org/10.1017/S0952523817000360 Published online by Cambridge University Press

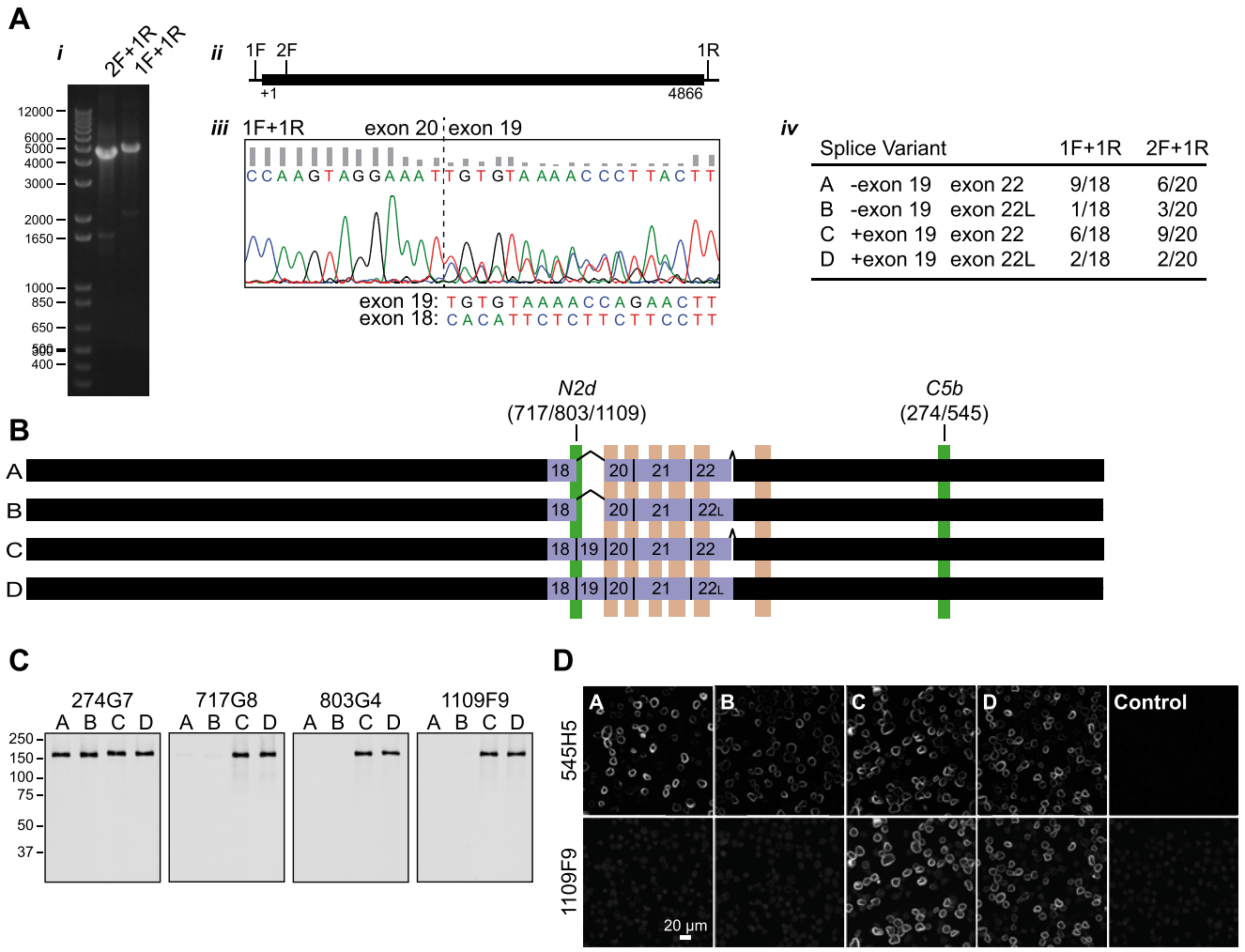


Fig. 5. Identification of TRPM1 splice variants in mouse retina. (**A**) (i) PCR of mouse retina cDNA. (ii) The open reading frame (4866 nt, thick line) and positions of primers are indicated. (iii) Sequencing electropherogram for PCR product 1F + 1R with a reverse primer, showing onset of heterogeneity at the exon 20–19 junction, with secondary peaks corresponding to the sequence of exon 18. The sequences expected for exons 19 and 18 (complimentary strand) are shown below. Similar results were obtained with the 2F + 1R PCR product. (iv) Summary of splice variants identified in the two PCR reactions. (**B**) Diagram of splice variants. The position of the mAb epitopes are indicated in green, and predicted transmembrane helices are shown in pink. Exons 18–22 are shown as purple boxes. (**C**, **D**) N2d mAbs specifically detect splice variants containing exon 19. (**C**) Purified recombinant isoforms were subjected to western blot with C5b mAb 274G7, and N2d mAbs 717G8, 803G4, and 1109F9. (**D**) Sf9 cells infected with recombinant baculovirus expressing TRPM1 isoforms, or a control virus expressing GST-nyctalopin, were double-labeled with 545H5 and 1109F9, followed by isotype-specific secondary antibodies.

(Fig. 4C), providing useful reagents for double labeling experiments. Notably, 274G7 and 545H5, which efficiently label the dendritic tips, bind to C5b, while 717G8 and 1109F9, which have reduced dendritic tip labeling, both bind to N2d.

Identification of TRPM1 splice variants

Two possible explanations for the differential labeling of TRPM1 mAbs are that they detect different quaternary complexes and/or that they detect different isoforms. To address the latter possibility, we analyzed TRPM1 isoforms in mouse retina cDNA. PCR of full-length or near-full-length TRPM1 from retina cDNA yielded products of expected sizes (Fig. 5Ai, ii). Sequencing of the gel-purified PCR products revealed a mixed population: with a reverse primer, beginning at the exon 20–19 junction, the electropherogram contains significant secondary peaks corresponding to the exon 18 sequence, indicating a subset of molecules missing exon 19 (Fig. 5Aiii). Although no other region of the sequence contained obvious heterogeneity, preliminary sequencing of clones revealed the presence of an extended exon 22 (exon 22L) containing 18 extra bp at the 3′ end. The PCR products were cloned and analyzed for the presence of exons 19 and 22L by restriction digest (see Materials and methods). Among the 38 clones with restrictions consistent with full-length TRPM1, all four possible combinations were observed (Fig. 5Aiv). Two exemplars of each group were verified by sequencing. All studies to date involving heterologously expressed TRPM1 have apparently used variant C or its rat or human homolog (Oancea et al., 2009; Koike et al., 2010; Cao et al., 2011; Lambert et al., 2011; Shen et al., 2012) or N-terminally truncated versions thereof (Xu et al., 2001; Oancea et al., 2009). However, it is unknown which variants participate in the transduction channel or if they have different functions.

https://doi.org/10.1017/S0952523817000360 Published online by Cambridge University Press

Skipping exon 19 results in an in-frame deletion of 44 amino acids in the N-terminal arm near the transmembrane domain. Exon 19 overlaps with the N2d epitope (Fig. 5B), suggesting the possibility of isoform-specific detection by N2d mAbs. To test this, baculovirus-expressed TRPM1 isoforms were analyzed by western blotting (Fig. 5C) and IF (Fig. 5D). While the C5b mAbs detected all four isoforms as expected, the N2d mAbs only detected isoforms C and D, which contain exon 19.

Although exon 19 skipping was observed in 19 of our 38 retina cDNA clones, it does not appear to be a conserved feature. In a RNA-seq transcriptome study of human retina (Farkas et al., 2013), no reads spanning the putative exon 18–20 junction were detected (Fig. 6A). Furthermore, the conservation of exon 19 among vertebrates is similar to that of exons 18 and 20 (Fig. 6A). BLAST analysis of an independent human retina RNA-seq data set (from NCBI GEO accession GSE94437) found 1095 and 870 reads spanning the exon 18–19 and 19–20 junctions, respectively, but only 2 reads spanning the 18–20 junction. On the other hand, BLAST analysis of mouse retina RNA-seq data (Mustafi et al., 2011, 2016) found 184 reads spanning the exon 18–20 junction, 339 reads spanning the exon 18–19 junction, and 249 reads spanning the exon 19–20 junction (not shown). These data are consistent with exon 19 skipping in a large fraction of mouse retina transcripts but not in human retina transcripts.

Exon 22L results from use of an alternative downstream splice donor site, and encodes six extra amino acids (Arg-Lys-Thr-Arg-Ile-His) followed by a Leu→Ile change at the new junction, in the predicted pore loop region of TRPM1 (Figs. 5B, 6E and 6F). This insertion was present in 8 of the 38 clones and was also detected in a similar fraction of human retina transcripts in the RNA-seq study (Farkas et al., 2013), which detected 139 reads spanning the annotated exon 22–23 junction, as well as 41 reads spanning a novel junction corresponding to exon 22L–23 (Fig. 6B and 6C). The extended exon 22L has also been reported in a clone of rat TRPM1 (Lis et al., 2005). Furthermore, the splice donor sites which

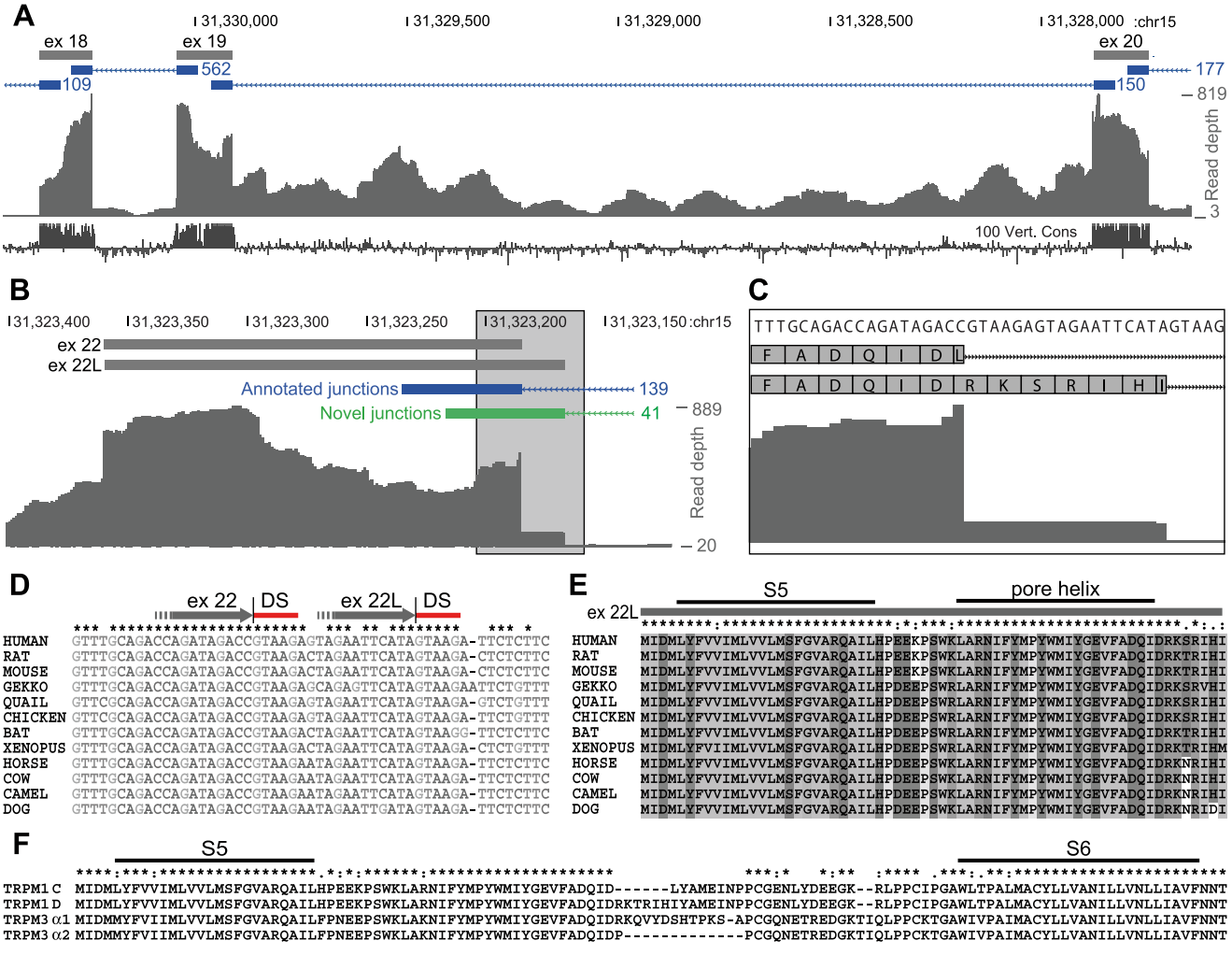


Fig. 6. Exon 22L is conserved, while exon 19 skipping is not. (**A–C**) Analysis of previously published human retina RNA-seq data (Farkas et al., 2013). (**A**) No reads spanning an exon 18–20 junction were detected, and exons 18, 19, and 20 are similarly conserved among vertebrates, suggesting that exon 19 skipping is not conserved. (**B**) 139 reads spanning the canonical exon 22–23 junction were detected (blue), as well as 41 reads spanning the exon 22L–23 junction (green). (**C**) Zoomed in view of the boxed region in (**B**). (**D**) Multiple sequence alignment of nucleotide sequences near the end of exon 22. The ends of exon 22 and 22L are shown as gray arrows, with splice donor sites (DS) indicated by red bars. Both donor sites are conserved, suggesting conservation of both exons 22 and 22L. (**E**) Multiple sequence alignment of exon 22L amino acid sequences. The predicted locations of the S5 transmembrane helix and pore helix are shown (Agosto et al., 2014). (**F**) Multiple sequence alignment of TRPM1 and TRPM3 isoforms. TRPM1(B/D) isoforms (containing exon 22L) and TRPM3 α1 have insertions in similar positions in the predicted pore loop.

https://doi.org/10.1017/S0952523817000360 Published online by Cambridge University Press

give rise to exons 22 and 22L are both well conserved, as are the predicted amino acid sequences (Fig. 6D and 6E).

Detection of TRPM1(A/B) isoform proteins

If all TRPM1 proteins in the retina contain exon 19, then quantitative western blots with any of the mAbs should yield the same result for the total amount of TRPM1 protein present. On the other hand, the presence of A/B isoform proteins (missing exon 19) should yield a reduced TRPM1 detection when using N2d mAbs. To determine whether A/B isoforms are present in the mouse retina, quantitative western blots of retina PNS samples, along with a standard curve of purified TRPM1(C), were performed with 545H5 and 1109F9 (Fig. 7A). Although the absolute quantification varied between experiments (between ~9 and ~14 ng/retina for 545H5 and ~6 and ~11 ng/retina for 1109F9), 1109F9 did yield a significantly reduced determination (~70–80%) compared to that of 545H5 (Fig. 7Aiii, iv), suggesting that ~20–30% of TRPM1 in mouse retina is missing exon 19.

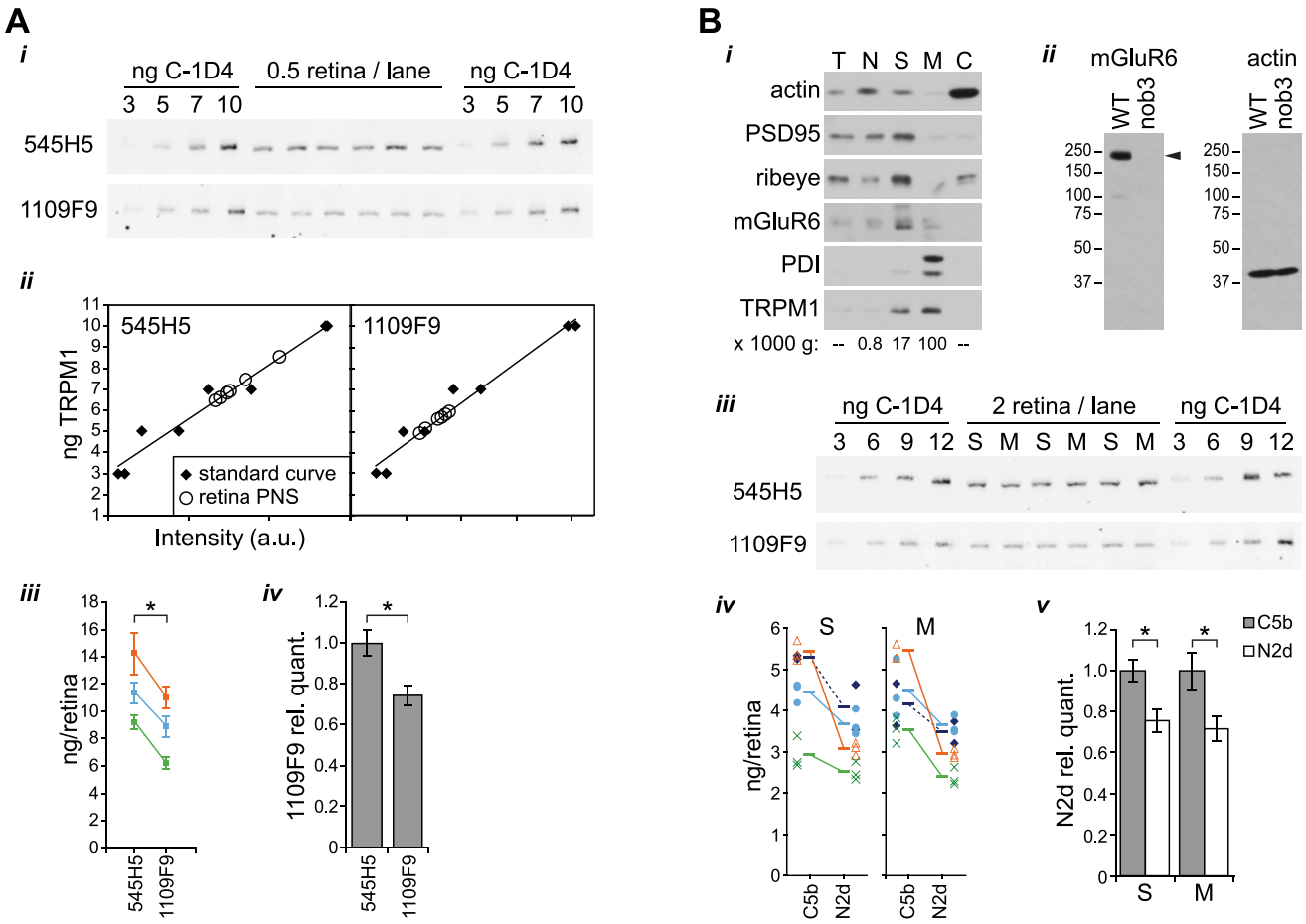


Fig. 7. TRPM1 isoforms lacking exon 19 are present in both cell bodies and dendritic tips. (**A**) Quantitative western blots of retina PNS and standard curves of purified isoform C were labeled with 545H5 or 1109F9. (i) Example western blots. Each experiment was performed with two identical gels that were transferred and blotted in parallel. Each gel contained duplicate standard curves and six technical replicates of retina sample. (ii) Example quantitation of the westerns shown in (i). (iii) Results from three experiments are shown. Points and error bars show means ±S.D. of the six technical replicates from each western blot. Values obtained in the same experiment are color-coded and connected by lines. *$P < 0.01$, paired t test with means only, not including technical replicates, $n = 3$. (iv) For each experiment, the 1109F9 quantification was divided by the value obtained with 545H5. Bars represents means ±S.D., calculated with error propagation; *$P < 0.01$, unpaired t test. (**B**) (i) Retinas were fractionated by differential centrifugation and equal amounts of total protein were loaded in each lane. Membranes were blotted for presynaptic markers PSD-95 and ribeye, postsynaptic marker mGluR6, ER marker PDI, and TRPM1 (using mAb 545H5). The relative force of centrifugation is indicated below the relevant lanes. T, total; N, nuclei; S, synaptosomes; M, microsomes; C, cytoplasm. (ii) Validation of the mGluR6 antibody. Whole retina lysates from WT and Grm6^{nob3} mice (~0.25 retina/lane) were blotted with mGluR6 or actin antibody. mGluR6 (arrowhead) is detected in WT, but not *nob3*, retina. The apparent molecular weight of nearly 250 kDa is significantly different from the predicted size of 95 kDa but is consistent with previously published western blots of mGluR6 (Orlandi et al., 2013; Cao et al., 2015). (iii) Quantitative westerns were performed as in (**A**), with three replicate lanes each for synaptosome (S) and microsome (M) fractions. (iv) Results from four experiments with either 545H5/1109F9 (solid lines) or 274G7/1109F9 (dashed lines) are shown. Points represent technical replicates, with each experiment represented by a different symbol. Means from each experiment are indicated by horizontal lines, and mean values obtained in the same experiment are connected by lines. (v) For each experiment, the N2d value was divided by the C5b value. Bars represent means ±S.D., calculated with error propagation; *$P < 0.005$, unpaired t test. All quantitative westerns were performed with fluorescent secondary antibodies and imaged with an Odyssey scanner.

https://doi.org/10.1017/S0952523817000360 Published online by Cambridge University Press

Since bipolar cell dendritic tips are poorly labeled by N2d mAbs, and N2d mAbs fail to detect A/B isoforms, we hypothesized that those isoforms might be enriched at the dendritic tips. To test this, retinas were fractionated by differential centrifugation to separate synaptosomes from other membrane-containing material (Fig. 7B). Fractions were probed with antibodies for the presynaptic marker ribeye, postsynaptic density 95 (PSD-95), which is presynaptic at the photoreceptor/bipolar cell synapse (Koulen et al., 1998), ER lumen resident protein disulfide isomerase (PDI), TRPM1, and mGluR6 (Fig. 7Bi). PSD-95, ribeye, and mGluR6 are enriched in the 17k pellet, consistent with the enrichment of synaptosomes containing ON bipolar cell dendritic tips. In contrast, PDI is enriched in the 100k pellet, consistent with the enrichment of microsomes including ER. TRPM1 is present in both fractions, as expected from its localization in both dendritic tips and cell bodies. Quantitative western blots were performed to compare the levels of A/B isoforms in synaptosome and microsome fractions (Fig. 7Biii–v). The ratio of TRPM1 determinations from the 1109F9 and 545H5 blots was similar in both fractions and also similar to the ratio observed with the whole retina PNS. This is contrary to the hypothesis that A/B isoforms are enriched at the dendritic tips and instead indicates that A/B isoforms are present in similar relative amounts in both the cell bodies and dendritic tips. The lack of isoform enrichment in the synaptosome fraction suggests that the differential detection of TRPM1 in the dendritic tips may be due to masking of the N2d epitope by a synapse-specific quaternary complex. However, the synaptosome and microsome fractions are not pure, so the possibility remains that there may be small differences in isoform levels which were not detected.

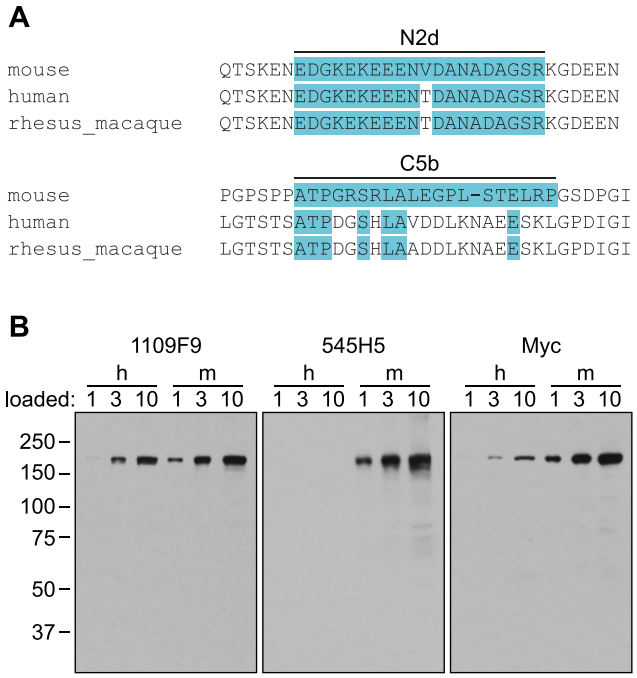


Fig. 8. Conservation of mAb epitopes. (**A**) Multiple sequence alignment of TRPM1 orthologs in the vicinity of the mAb epitopes. Amino acids identical to the mouse sequence are highlighted in blue. (**B**) Lysates from HEK-293 cells transfected with Myc-tagged mouse (m) or human (h) TRPM1 were blotted with 1109F9, 545H5, or anti-Myc; human TRPM1 is detected with 1109F9 but not 545H5. The number above each lane indicates the relative amount of lysate loaded.

Conservation of mAb epitopes

The N2d epitope and surrounding region are fairly well conserved, while the C5b epitope is not (Fig. 8A). To test the ability of the mAbs to detect human TRPM1, western blots were performed with HEK cells transfected with Myc-tagged mouse or human TRPM1 (Fig. 8B). The N2d mAb 1109F9 detects both mouse and human proteins expressed in HEK cells, while the C5b mAb 545H5 only detects the mouse protein. These results are consistent with the conservation of the N2d epitope and suggest that N2d mAbs may be useful reagents for detecting TRPM1 in western blots in various model systems.

Discussion

In this study, we report antibody-based identification of two distinct pools of TRPM1 in retinal bipolar cells. mAbs binding to an epitope in the C-terminal arm detected TRPM1 in both cell bodies and dendritic tips, while mAbs binding to an epitope (N2d) in the N-terminal arm near the transmembrane domain preferentially detected TRPM1 in cell bodies (see Figs. 2–4). One explanation for these data is complex formation in the dendritic tips leading to epitope masking. Formation of synapse-specific complexes is not surprising, as other proteins reported to participate in the mGluR6 cascade are specifically localized to the dendritic tips (Nomura et al., 1994; Masu et al., 1995; Morgans et al., 2006; Gregg et al., 2007; Peachey et al., 2012; Orlandi et al., 2013; Zeitz et al., 2013; Neuillé et al., 2015), and the transduction channel function ascribed to TRPM1 (Morgans et al., 2009; Shen et al., 2009, 2012; Koike et al., 2010) is likely limited to TRPM1 molecules localized at the photoreceptor-bipolar cell synapse. The proximity of the N2d epitope to the transmembrane domain may also limit its ability to bind to TRPM1 in the context of complex formation involving other membrane proteins. The significance of the additional TRPM1 localized throughout the dendrites and cell bodies (see for example Figs. 1 and 2) is unknown; those proteins may be immature complexes or trafficking intermediates, and/or they may possibly mediate other functions.

We identified several splice variants in mouse retina, including variants lacking exon 19, which overlaps with the N2d epitope and is required for detection by N2d mAbs (see Fig. 5). Although no enrichment of isoforms lacking exon 19 was detected in the synaptosome fraction (see Fig. 7), our data do not permit ruling out the possibility of small differences in the relative levels of isoforms, which could contribute to the differential labeling in IF.

The significance of TRPM1 splice variants is unknown. The observation that isoforms lacking exon 19 were not detectably enriched at the dendritic tips, along with the fact that skipping exon 19 does not appear to be a conserved feature (see Fig. 6), suggests that these isoforms do not have a specific function in signal transduction. On the other hand, the conservation of exon 22L and its location in the predicted pore loop suggest that it may confer physiologically relevant functional properties. In fact, TRPM3, the closest relative of TRPM1, has splice variants differing by an insertion in a similar region (Fig. 6F) that have different channel properties (Oberwinkler et al., 2005).

Clearly, the TRPM1 population in ON-BPCs is structurally and functionally heterogenous: in addition to any posttranslational modifications, about which nothing is known, there are different polypeptides encoded by different splice variants, as well as different complexes in different locations. Understanding the properties of these and the relationships among them will be essential for a full understanding of TRPM1 function.

https://doi.org/10.1017/S0952523817000360 Published online by Cambridge University Press

Acknowledgments

This work was supported by National Institutes of Health grants R01-EY007981/EY007981-S1 (to T.G.W.), F32 EY200672 (to M.A.A.), and F32 EY024815 (to I.A.A.), by a Knights Templar Eye Foundation Pediatric Ophthalmology Career-Starter Grant (to M.A.A.), by the Welch Foundation (Q0035), and by the Monoclonal Antibody/Recombinant Protein Expression Shared Resource at Baylor College of Medicine with funding from NIH Cancer Center Support Grant P30 CA125123.

References

Agosto, M.A., Zhang, Z., He, F., Anastassov, I.A., Wright, S.J., McGehee, J. & Wensel, T.G. (2014). Oligomeric state of purified transient receptor potential melastatin-1 (TRPM1), a protein essential for dim light vision. *Journal of Biological Chemistry* **289**, 27019–27033.

Audo, I., Kohl, S., Leroy, B.P., Munier, F.L., Guillonneau, X., Mohand-Said, S., Bujakowska, K., Nandrot, E.F., Lorenz, B., Preising, M., Kellner, U., Renner, A.B., Bernd, A., Antonio, A., Moskova-Doumanova, V., Lancelot, M., Poloschek, C.M., Drumare, I., Defoort-Dhellemmes, S., Wissinger, B., Leveillard, T., Hamel, C.P., Schorderet, D.F., De Baere, E., Berger, W., Jacobson, S.G., Zrenner, E., Sahel, J-A., Bhattacharya, S.S. & Zeitz, C. (2009). *TRPM1* is mutated in patients with autosomal-recessive complete congenital stationary night blindness. *The American Journal of Human Genetics* **85**, 720–729.

Audo, I., Bujakowska, K., Orhan, E., Poloschek, C.M., Defoort-Dhellemmes, S., Drumare, I., Kohl, S., Luu, T.D., Lecompte, O., Zrenner, E., Lancelot, M-E., Antonio, A., Germain, A., Michiels, C., Audier, C., Letexier, M., Saraiva, J-P., Leroy, B.P., Munier, F.L., Mohand-Saïd, S., Lorenz, B., Friedburg, C., Preising, M., Kellner, U., Renner, A.B., Moskova-Doumanova, V., Berger, W., Wissinger, B., Hamel, C.P., Schorderet, D.F., De Baere, E., Sharon, D., Banin, E., Jacobson, S.G., Bonneau, D., Zanlonghi, X., Le Meur, G., Casteels, I., Koenekoop, R., Long, V.W., Meire, F., Prescott, K., de Ravel, T., Simmons, I., Nguyen, H., Dollfus, H., Poch, O., Léveillard, T., Nguyen-Ba-Charvet, K., Sahel, J-A., Bhattacharya, S.S. & Zeitz, C. (2012). Whole-exome sequencing identifies mutations in *GPR179* leading to autosomal-recessive complete congenital stationary night blindness. *The American Journal of Human Genetics* **90**, 321–330.

Bech-Hansen, N.T., Naylor, M.J., Maybaum, T.A., Sparkes, R.L., Koop, B., Birch, G., Bergen, A.A.B., Prinsen, C.F.M., Polomeno, R.C., Gal, A., Drack, A.V., Musarella, M.A., Jacobson, S.G., Young, R.S.L. & Weleber, R.G. (2000). Mutations in *NYX*, encoding the leucine-rich proteoglycan nyctalopin, cause X-linked complete congenital stationary night blindness. *Nature Genetics* **26**, 319–323.

Cao, Y., Pahlberg, J., Sarria, I., Kamasawa, N., Sampath, A.P. & Martemyanov, K.A. (2012). Regulators of G protein signaling RGS7 and RGS11 determine the onset of the light response in ON bipolar neurons. *Proceedings of the National Academy of Sciences of the United States of America* **109**, 7905–7910.

Cao, Y., Posokhova, E. & Martemyanov, K.A. (2011). TRPM1 forms complexes with nyctalopin *in vivo* and accumulates in postsynaptic compartment of ON-bipolar meurons in mGluR6-dependent manner. *Journal of Neuroscience* **31**, 11521–11526.

Cao, Y., Sarria, I., Fehlhaber, K.E., Kamasawa, N., Orlandi, C., James, K.N., Hazen, J.L., Gardner, M.R., Farzan, M., Lee, A., Baker, S., Baldwin, K., Sampath, A.P. & Martemyanov, K.A. (2015). Mechanism for selective synaptic wiring of rod photoreceptors into the retinal circuitry and its role in vision. *Neuron* **87**, 1248–1260.

Chen, C-K., Eversole-Cire, P., Zhang, H., Mancino, V., Chen, Y-J., He, W., Wensel, T.G. & Simon, M.I. (2003). Instability of GGL domain-containing RGS proteins in mice lacking the G protein β-subunit $G\beta_5$. *Proceedings of the National Academy of Sciences of the United States of America* **100**, 6604–6609.

Dhingra, A., Faurobert, E., Dascal, N., Sterling, P. & Vardi, N. (2004). A retinal-specific regulator of G-protein signaling interacts with $G\alpha_o$ and accelerates an expressed metabotropic glutamate receptor 6 cascade. *Journal of Neuroscience* **24**, 5684–5693.

Dhingra, A., Jiang, M., Wang, T-L., Lyubarsky, A., Savchenko, A., Bar-Yehuda, T., Sterling, P., Birnbaumer, L. & Vardi, N. (2002). Light response of retinal ON bipolar cells requires a specific splice variant of $G\alpha_o$. *Journal of Neuroscience* **22**, 4878–4884.

Dhingra, A., Lyubarsky, A., Jiang, M., Pugh, E.N., Birnbaumer, L., Sterling, P. & Vardi, N. (2000). The light response of ON bipolar neurons requires $G\alpha_o$. *Journal of Neuroscience* **20**, 9053–9058.

Dhingra, A., Ramakrishnan, H., Neinstein, A., Fina, M.E., Xu, Y., Li, J., Chung, D.C., Lyubarsky, A. & Vardi, N. (2012). $G\beta_3$ is required for normal light ON responses and synaptic maintenance. *Journal of Neuroscience* **32**, 11343–11355.

Dryja, T.P., McGee, T.L., Berson, E.L., Fishman, G.A., Sandberg, M.A., Alexander, K.R., Derlacki, D.J. & Rajagopalan, A.S. (2005). Night blindness and abnormal cone electroretinogram ON responses in patients with mutations in the *GRM6* gene encoding mGluR6. *Proceedings of the National Academy of Sciences of the United States of America* **102**, 4884–4889.

Farkas, M.H., Grant, G.R., White, J.A., Sousa, M.E., Consugar, M.B. & Pierce, E.A. (2013). Transcriptome analyses of the human retina identify unprecedented transcript diversity and 3.5 Mb of novel transcribed sequence via significant alternative splicing and novel genes. *BMC Genomics* **14**, 486.

Gilliam, J.C. & Wensel, T.G. (2011). TRP channel gene expression in the mouse retina. *Vision Research* **51**, 2440–2452.

Gimenez, E. & Montoliu, L. (2001). A simple polymerase chain reaction assay for genotyping the retinal degeneration mutation (Pdeb rd1) in FVB/N-derived transgenic mice. *Laboratory Animals* **35**, 153–156.

Gregg, R.G., Kamermans, M., Klooster, J., Lukasiewicz, P.D., Peachey, N.S., Vessey, K.A. & McCall, M.A. (2007). Nyctalopin expression in retinal bipolar cells restores visual function in a mouse model of complete X-linked congenital stationary night blindness. *Journal of Neurophysiology* **98**, 3023–3033.

Gregg, R.G., Mukhopadhyay, S., Candille, S.I., Ball, S.L., Pardue, M.T., McCall, M.A. & Peachey, N.S. (2003). Identification of the gene and the mutation responsible for the mouse *nob* phenotype. *Investigative Ophthalmology & Visual Science* **44**, 378–384.

Harper, J.W., Adami, G.R., Wei, N., Keyomarsi, K. & Elledge, S.J. (1993). The p21 Cdk-interacting protein Cip1 is a potent inhibitor of G1 cyclin-dependent kinases. *Cell* **75**, 805–816.

Koike, C., Obara, T., Uriu, Y., Numata, T., Sanuki, R., Miyata, K., Koyasu, T., Ueno, S., Funabiki, K., Tani, A., Ueda, H., Kondo, M., Mori, Y., Tachibana, M. & Furukawa, T. (2010). TRPM1 is a component of the retinal ON bipolar cell transduction channel in the mGluR6 cascade. *Proceedings of the National Academy of Sciences of the United States of America* **107**, 332–337.

Koulen, P., Fletcher, E.L., Craven, S.E., Bredt, D.S. & Wassle, H. (1998). Immunocytochemical localization of the postsynaptic density protein PSD-95 in the mammalian retina. *Journal of Neuroscience* **18**, 10136–10149.

Laemmli, U.K. (1970). Cleavage of structural proteins during the assembly of the head of bacteriophage T4. *Nature* **227**, 680–685.

Lambert, S., Drews, A., Rizun, O., Wagner, T.F.J., Lis, A., Mannebach, S., Plant, S., Portz, M., Meissner, M., Philipp, S.E. & Oberwinkler, J. (2011). Transient receptor potential melastatin 1 (TRPM1) is an ion-conducting plasma membrane channel inhibited by zinc. *Journal of Biological Chemistry* **286**, 12221–12233.

Larkin, M.A., Blackshields, G., Brown, N.P., Chenna, R., McGettigan, P.A., McWilliam, H., Valentin, F., Wallace, I.M., Wilm, A., Lopez, R., Thompson, J.D., Gibson, T.J. & Higgins, D.G. (2007). Clustal W and Clustal X version 2.0. *Bioinformatics* **23**, 2947–2948.

Li, Z., Sergouniotis, P.I., Michaelides, M., Mackay, D.S., Wright, G.A., Devery, S., Moore, A.T., Holder, G.E., Robson, A.G. & Webster, A.R. (2009). Recessive mutations of the gene *TRPM1* abrogate ON bipolar cell function and cause complete congenital stationary night blindness in humans. *The American Journal of Human Genetics* **85**, 711–719.

Lis, A., Wissenbach, U. & Philipp, S.E. (2005). Transcriptional regulation and processing increase the functional variability of TRPM channels. *Naunyn-Schmiedeberg's Archives of Pharmacology* **371**, 315–324.

Mackenzie, D., Arendt, A., Hargrave, P., McDowell, J.H. & Molday, R.S. (1984). Localization of binding sites for carboxyl terminal specific anti-rhodopsin monoclonal antibodies using synthetic peptides. *Biochemistry* **23**, 6544–6549.

Maddox, D.M., Vessey, K.A., Yarbrough, G.L., Invergo, B.M., Cantrell, D.R., Inayat, S., Balannik, V., Hicks, W.L., Hawes, N.L., Byers, S., Smith, R.S., Hurd, R., Howell, D., Gregg, R.G., Chang, B.,

https://doi.org/10.1017/S0952523817000360 Published online by Cambridge University Press

Naggert, J.K., Troy, J.B., Pinto, L.H., Nishina, P.M. & McCall, M.A. (2008). Allelic variance between GRM6 mutants, *Grm6^{nob3}* and *Grm6^{nob4}* results in differences in retinal ganglion cell visual responses. *The Journal of Physiology* **586**, 4409–4424.

Masu, M., Iwakabe, H., Tagawa, Y., Miyoshi, T., Yamashita, M., Fukuda, Y., Sasaki, H., Hiroi, K., Nakamura, Y., Shigemoto, R., Takada, M., Nakamura, K., Nakao, K., Katsuki, M. & Nakanishi, S. (1995). Specific deficit of the ON response in visual transmission by targeted disruption of the mGluR6 gene. *Cell* **80**, 757–765.

Mattapallil, M.J., Wawrousek, E.F., Chan, C-C., Zhao, H., Roychoudhury, J., Ferguson, T.A. & Caspi, R.R. (2012). The *rd8* mutation of the *Crb1* gene is present in vendor lines of C57BL/6N mice and embryonic stem cells, and confounds ocular induced mutant phenotypes. *Investigative Ophthalmology & Visual Science* **53**, 2921–2927.

Mojumder, D.K., Qian, Y. & Wensel, T.G. (2009). Two R7 regulator of G-protein signaling proteins shape retinal bipolar cell signaling. *Journal of Neuroscience* **29**, 7753–7765.

Morgans, C.W., Ren, G. & Akileswaran, L. (2006). Localization of nyctalopin in the mammalian retina. *European Journal of Neuroscience* **23**, 1163–1171.

Morgans, C.W., Zhang, J., Jeffrey, B.G., Nelson, S.M., Burke, N.S., Duvoisin, R.M. & Brown, R.L. (2009). TRPM1 is required for the depolarizing light response in retinal ON-bipolar cells. *Proceedings of the National Academy of Sciences of the United States of America* **106**, 19174–19178.

Mustafi, D., Kevany, B.M., Bai, X., Golczak, M., Adams, M.D., Wynshaw-Boris, A. & Palczewski, K. (2016). Transcriptome analysis reveals rod/cone photoreceptor specific signatures across mammalian retinas. *Human Molecular Genetics* **25**, 4376–4388.

Mustafi, D., Kevany, B.M., Genoud, C., Okano, K., Cideciyan, A.V., Sumaroka, A., Roman, A.J., Jacobson, S.G., Engel, A., Adams, M.D. & Palczewski, K. (2011). Defective photoreceptor phagocytosis in a mouse model of enhanced S-cone syndrome causes progressive retinal degeneration. *The FASEB Journal* **25**, 3157–3176.

Nakajima, Y., Iwakabe, H., Akazawa, C., Nawa, H., Shigemoto, R., Mizuno, N. & Nakanishi, S. (1993). Molecular characterization of a novel retinal metabotropic glutamate receptor mGluR6 with a high agonist selectivity for L-2-amino-4-phosphonobutyrate. *Journal of Biological Chemistry* **268**, 11868–11873.

Neuillé, M., Morgans, C.W., Cao, Y., Orhan, E., Michiels, C., Sahel, J-A., Audo, I., Duvoisin, R.M., Martemyanov, K.A. & Zeitz, C. (2015). LRIT3 is essential to localize TRPM1 to the dendritic tips of depolarizing bipolar cells and may play a role in cone synapse formation. *European Journal of Neuroscience* **42**, 1966–1975.

Neuillé, M., El Shamieh, S., Orhan, E., Michiels, C., Antonio, A., Lancelot, M-E., Condroyer, C., Bujakowska, K., Poch, O., Sahel, J-A., Audo, I. & Zeitz, C. (2014). *Lrit3* deficient mouse (*nob6*): A novel model of complete congenital stationary night blindness (cCSNB). *PLos One* **9**, e90342.

Nomura, A., Shigemoto, R., Nakamura, Y., Okamoto, N., Mizuno, N. & Nakanishi, S. (1994). Developmentally regulated postsynaptic localization of a metabotropic glutamate receptor in rat rod bipolar cells. *Cell* **77**, 361–369.

Oancea, E., Vriens, J., Brauchi, S., Jun, J., Splawski, I. & Clapham, D.E. (2009). TRPM1 forms ion channels associated with melanin content in melanocytes. *Science Signaling* **2**, ra21.

Oberwinkler, J., Lis, A., Giehl, K.M., Flockerzi, V. & Philipp, S.E. (2005). Alternative splicing switches the divalent cation selectivity of TRPM3 channels. *Journal of Biological Chemistry* **280**, 22540–22548.

Orlandi, C., Cao, Y. & Martemyanov, K.A. (2013). Orphan receptor GPR179 forms macromolecular complexes with components of metabotropic signaling cascade in retina ON-bipolar neurons. *Investigative Ophthalmology & Visual Science* **54**, 7153–7161.

Peachey, N.S., Ray, T.A., Florijn, R., Rowe, L.B., Sjoerdsma, T., Contreras-Alcantara, S., Baba, K., Tosini, G., Pozdeyev, N., Iuvone, P.M., Bojang, P., Pearring, J.N., Simonsz, H.J., van Genderen, M., Birch, D.G., Traboulsi, E.I., Dorfman, A., Lopez, I., Ren, H., Goldberg, A.F.X., Nishina, P.M., Lachapelle, P., McCall, M.A., Koenekoop, R.K., Bergen, A.A.B., Kamermans, M. & Gregg, R.G. (2012). GPR179 is required for depolarizing bipolar cell function and is mutated in autosomal-recessive complete congenital stationary night blindness. *The American Journal of Human Genetics* **90**, 331–339.

Pearring, J.N., Bojang, P. Jr., Shen, Y., Koike, C., Furukawa, T., Nawy, S. & Gregg, R.G. (2011). A role for nyctalopin, a small leucine-rich repeat protein, in localizing the TRP melastatin 1 channel to retinal depolarizing bipolar cell dendrites. *Journal of Neuroscience* **31**, 10060–10066.

Pusch, C.M., Zeitz, C., Brandau, O., Pesch, K., Achatz, H., Feil, S., Scharfe, C., Maurer, J., Jacobi, F.K., Pinckers, A., Andreasson, S., Hardcastle, A., Wissinger, B., Berger, W. & Meindl, A. (2000). The complete form of X-linked congenital stationary night blindness is caused by mutations in a gene encoding a leucine-rich repeat protein. *Nature Genetics* **26**, 324–327.

Rao, A., Dallman, R., Henderson, S. & Chen, C-K. (2007). $G\beta_5$ Is required for normal light responses and morphology of retinal ON-bipolar cells. *Journal of Neuroscience* **27**, 14199–14204.

Ray, T.A., Heath, K.M., Hasan, N., Noel, J.M., Samuels, I.S., Martemyanov, K.A., Peachey, N.S., McCall, M.A. & Gregg, R.G. (2014). GPR179 Is required for high sensitivity of the mGluR6 signaling cascade in depolarizing bipolar cells. *Journal of Neuroscience* **34**, 6334–6343.

Scott, D.B., Blanpied, T.A. & Ehlers, M.D. (2003). Coordinated PKA and PKC phosphorylation suppresses RXR-mediated ER retention and regulates the surface delivery of NMDA receptors. *Neuropharmacology* **45**, 755–767.

Shen, Y., Heimel, J.A., Kamermans, M., Peachey, N.S., Gregg, R.G. & Nawy, S. (2009). A transient receptor potential-like channel mediates synaptic transmission in rod bipolar cells. *Journal of Neuroscience* **29**, 6088–6093.

Shen, Y., Rampino, M.A.F., Carroll, R.C. & Nawy, S. (2012). G-protein–mediated inhibition of the Trp channel TRPM1 requires the $G\beta_\gamma$ dimer. *Proceedings of the National Academy of Sciences of the United States of America* **109**, 8752–8757.

Shim, H., Wang, C-T., Chen, Y-L., Chau, V.Q., Fu, K.G., Yang, J., McQuiston, A.R., Fisher, R.A. & Chen, C-K. (2012). Defective retinal depolarizing bipolar cells in regulators of G protein signaling (RGS) 7 and 11 double null mice. *Journal of Biological Chemistry* **287**, 14873–14879.

Sievers, F., Wilm, A., Dineen, D., Gibson, T.J., Karplus, K., Li, W., Lopez, R., McWilliam, H., Remmert, M., Soding, J., Thompson, J.D. & Higgins, D.G. (2011). Fast, scalable generation of high-quality protein multiple sequence alignments using Clustal Omega. *Molecular Systems Biology* **7**, 539.

Van Genderen, M.M., Bijveld, M.M.C., Claassen, Y.B., Florijn, R.J., Pearring, J.N., Meire, F.M., Mccall, M.A., Riemslag, F.C.C., Gregg, R.G., Bergen, A.A.B. & Kamermans, M. (2009). Mutations in *TRPM1* are a common cause of complete congenital stationary night blindness. *The American Journal of Human Genetics* **85**, 730–736.

VanGuilder, H.D., Brucklacher, R.M., Patel, K., Ellis, R.W., Freeman, W.M. & Barber, A.J. (2008). Diabetes downregulates presynaptic proteins and reduces basal synapsin I phosphorylation in rat retina. *European Journal of Neuroscience* **28**, 1–11.

Xu, X.S., Moebius, F., Gill, D.L. & Montell, C. (2001). Regulation of melastatin, a TRP-related protein, through interaction with a cytoplasmic isoform. *Proceedings of the National Academy of Sciences of the United States of America* **98**, 10692–10697.

Zeitz, C., van Genderen, M., Neidhardt, J., Luhmann, U.F.O., Hoeben, F., Forster, U., Wycisk, K., Mátyás, G., Hoyng, C.B., Riemslag, F., Meire, F., Cremers, F.P.M. & Berger, W. (2005). Mutations in *GRM6* cause autosomal recessive congenital stationary night blindness with a distinctive scotopic 15 Hz flicker electroretinogram. *Investigative Ophthalmology & Visual Science* **46**, 4328–4335.

Zeitz, C., Jacobson, S.G., Hamel, C.P., Bujakowska, K., Neuille, M., Orhan, E., Zanlonghi, X., Lancelot, M., Michiels, C., Schwartz, S.B., Bocquet, B., Antonio, A., Audier, C., Letexier, M., Saraiva, J., Luu, T.D., Sennlaub, F., Nguyen, H., Lecompte, O., Poch, O., Dollfus, H., Kohl, S., Sahel, J-A., Bhattacharya, S.S. & Audo, I. (2013). Whole-exome sequencing identifies *LRIT3* mutations as a cause of autosomal-recessive complete congenital stationary night blindness. *The American Journal of Human Genetics* **92**, 67–75.

https://doi.org/10.1017/S0952523817000360 Published online by Cambridge University Press